

Self-assembly of protein amyloids: a competition between amorphous and ordered aggregation

Chiu Fan Lee*

Physics Department, Clarendon Laboratory, Oxford University, Parks Road, Oxford OX1 3PU, UK

(Dated: November 27, 2019)

Protein aggregation in the form of a fibril, or protein amyloid, has important biological and technological implications. Although the self-assembly process is highly efficient, aggregates not in the fibrillar form would also occur and it is important to include these disordered species when discussing the thermodynamic equilibrium behaviour of the system. Here, we initiate such a task by considering a mixture of monomeric proteins and the corresponding aggregates in the disordered form (micelles) and in the fibrillar form (amyloid fibrils). By investigating the entropic and energetic components of the various species, we gain an understanding of the many empirical observations concerning the various amyloid promoting factors and the structural commonality among amyloids formed by different proteins. In particular, we demonstrate how aromatic residues contribute to amyloid formation in three different manners: i) high hydrophobicity, ii) π -stacking interaction along the fibrillar axis, and iii) high volume. Furthermore, by incorporating physiologically relevant parameters into our toy model, we explain why it is of relative ease to induce amyloid formation in many proteins and why it is energetically important to have multi-layer cross-beta structures. We then analyze how the formalism developed allows us to gain insight on the kinetic process of fibril formation.

PACS numbers: 82.35.Pq, 87.14.ef, 46.25.Cc, 87.19.xh

I. INTRODUCTION

Amyloids are insoluble fibrous protein aggregations stabilized by a network of hydrogen bonds and hydrophobic interactions [1, 2, 3, 4]. They are intimately related to many neurodegenerative diseases such as the Alzheimer's Disease, the Parkinson Disease and other prion diseases [5]. Better characterization of the various properties of amyloid fibrils is therefore of high importance for the understanding of the associated pathogenesis. More recently, viewing the protein amyloid formation as a highly efficient self-assembly process, possible applications have also been proposed, which, e.g., includes nanowire templating [6]. Given the high importance of protein amyloid in biology and potentially in technology, it is being studied intensively. For instance, much effort has been spent on investigating the amino-acid dependency on amyloid propensity [7, 8, 9, 10, 11, 12, 13]; the possibility of primary-sequence-based amyloid propensity predictions [14, 15, 16, 17, 18, 19]; the mechanical properties of protein amyloid [20, 21, 22]; the kinetics of amyloid formation [23, 24, 25, 26, 27, 28, 29, 30]; as well as the thermodynamical behaviours of the aggregation process [31, 32, 33, 34].

In this paper, we study protein amyloid self-assembly process at thermal equilibrium and deduce the *dominance* diagram with respect to the aggregating behavior. Specifically, we consider the thermodynamic behaviour of a mixture of monomers, aggregates with a linearly ordered structure (fibrils) and aggregates with a disor-

dered structure (a micelle-like aggregate). In the process, we gain an understanding on the amyloid propensity observed empirically with respect to the variations in the sequence charge, hydrophobicity, aromatic side chains content and hydrophobic pattern. In particular, our study suggests that aromatic interaction has a fibrillar stabilising effect other than its heightened hydrophobicity. Hence, our work contributes to the debate on whether the π -stacking interaction is an important contribution to fibril stability [7, 8, 9, 10, 11, 12]. We then employ the formalism to study the kinetic process of aggregation and discuss the different pathways of amyloid formation.

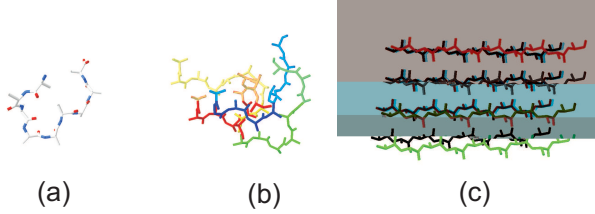
In Section II, we introduce our model of the protein self-assembly system and the concept of dominance diagram. In Section III, we discuss the behaviour of the system in the parameters regime that is experimentally relevant. In Section IV, we extend our simple model to include the considerations of the native state and the effect of pressure. In Section V, a discussion of the kinetic of self-assembly based on our free energy picture is presented. To fix notation and to be self-contained, we have derived all the major formula in the Appendix.

II. THE MODEL

We model a protein as a linear chain with the possibility of forming directional bonds (e.g., hydrogen bonds) and undirectional bonds (e.g., hydrophobic interactions). In this section, we will assume that these bonds are only possible between two different proteins. In other words, we assume that the distant parts of a protein do not interact. We also assume that there is no interaction between

*Electronic address: C.Lee1@physics.ox.ac.uk

FIG. 1: Schematic diagrams of the three species considered in this paper: (a) a monomeric protein in solution; (b) a micelle, or an amorphous aggregate, of four monomers; (c) an eight-monomer segment of an amyloid fibril consisting of two cross-beta structures (one cross-beta structure is coloured, the other is black). The hydrogen bonds stabilise the beta sheets in the vertical direction (not shown in this figure). (Drawn with DeepView [35].)



the protein and solution. With these assumptions, a free protein is always in the random coil state. We will extend these restrictions later in Section IV. Although the assumption seems unrealistic, it should be relevant to the many experiments performed on short model peptides.

Besides free proteins, we will consider two different types of aggregates: i) linearly structured aggregates (amyloid fibrils) and ii) disordered aggregates (micelles) (c.f. Fig. 1). For the micellar species, we assume that there is an optimal configuration consisting of M proteins. For the fibrillar species, we assume that the only ordered structure is made of stacking two cross-beta structures (c.f. Fig. 1c). We note that amyloid fibrils can exhibit structural variations even when prepared under the same condition, and the precise structural details will be highly primary sequence dependent (see, e.g., [36]).

Now a note on terminology: we will call a free protein in solution a monomer, a micelle consisting of h proteins a h -mer micelle, and a fibril consisting of k proteins a k -mer fibril.

Given the three different species: monomers, micelles and fibrils, we are interested in determining the dominant species, in terms of their relative abundancy in the solution. Denoting the free energy density for the monomeric species by η , that of a h -mer micelle by γ_h , and that of a k -mer fibril by f_k , at thermal equilibrium, the volume fractions of the various species are completely determined by the differences of these free energy densities (c.f. Appendix A.4).

For the monomers, as it is assumed that there is no interaction between the protein and the solution, or among the distant parts of the protein, η consists only of entropic contributions and can be expressed as follows (c.f. Eq. A14 in A 1):

$$\eta = -\frac{1}{\beta} [\log(\kappa v_a) + \log(\omega \Theta_a) + \log(s_a) - \beta P v_a]. \quad (1)$$

In the above expression, the first term denotes the entropic contribution coming from the translational freedom with respect to the centre of mass, the second term

is from the rotational freedom with respect to the centre of mass, the third term is from the flexible nature of the protein, i.e., the translational freedoms of every atom in the protein once the centre of mass and the principal axes are fixed. The fourth term is from the volume expansion/contraction contribution (see A 1 for the precise definitions of the parameters appeared).

For an amphiphilic protein with sufficiently hydrophobic portions, hydrophobic interaction would drive different copies of proteins to aggregate. The kinetically most accessible type of aggregation would be amorphous, i.e., structureless. This constitutes the micellar species that we consider now. In terms of free energy, these aggregates are the most difficult to handle analytically as the lack of structure renders it highly dependent on the primary sequence of the protein concerned. As a first approximation, we make the assumption that the free energy density can be described by a quadratic function with a unique minimum corresponding to an M -aggregate (c.f. Ch. 9 in [37]) where M is in the order of a few tens of proteins [24]. The free energy can thus be written as:

$$\gamma_k = \gamma_M + \Lambda(k - M)^2 \quad (2)$$

with

$$\Lambda \equiv \frac{\eta - \gamma_M}{(M - 1)^2}, \quad (3)$$

and γ_M is derived in Eq. A18:

$$\begin{aligned} \gamma_M = & -\frac{1}{\beta M} \left\{ \log[\kappa^M v_b \nu^{M-1}] + \log[\omega^M \Theta_b^M \xi_b^{M-1}] \right. \\ & \left. + M \log(s_b) - \beta P M v_b + M \beta \epsilon_b \right\}. \end{aligned} \quad (4)$$

In the above expression, besides the translational, rotational, configurational and volume terms as in Eq. 1, we also have a new bonding energy term, in which ϵ_b is the average energy gained per protein for being part of the micelle. Since micellar aggregates are assumed to have no rigid structure, ϵ_b would consist of mostly structurally less constraining interactions, such as general hydrophobic interactions, ionic bonds and other side-side interactions, and it would consist less of cross-peptide-backbone hydrogen bonds as found in fibrils.

The last species we are concerned with is the fibrillar (ordered) aggregates. For the k -aggregates, we have the following free energy density (c.f. Eq. A21 in the Appendix):

$$\begin{aligned} f_k = & -\frac{1}{\beta k} \left\{ \log[\kappa^k v_c \nu_c^{k-1}] + \log[\omega^k \Theta_c^k \xi_c^{k-1}] \right. \\ & \left. + (k - 2)\beta \epsilon_c + k \log(s_c) - \beta P k v_c \right\}. \end{aligned} \quad (5)$$

Similar to the micellar case, ϵ_c is the average energy gained per protein for becoming part of a fibril.

With the expressions for the free energy densities, we are now ready to discuss the relevant dominance of the species in terms of volume fractions (c.f. Appendix A.4). For the fibrillar species, f_k are monotonically decreasing and so $\max_k(f_k) = f_\infty$. We therefore find that $\max_k(f_k) < \eta$ if and only if:

$$\beta\epsilon_c > \log\left(\frac{v_a\Theta_a s_a}{\xi_c\nu_c\Theta_c s_c}\right) + \beta P(v_c - v_a) . \quad (6)$$

Similarly, $\gamma_M < \eta$ if and only if:

$$\beta\epsilon_b > \log\left(\frac{v_a\Theta_a s_a}{\xi_b\nu_b\Theta_b s_b}\right) + \beta P(v_b - v_a) , \quad (7)$$

where we have again ignored terms of order $1/M$ and approximated terms of order $(M-1)/M$ by 1 in the above inequality. This is a good approximation for $M \geq 30$, which we believe is the regime of interest for us here [24].

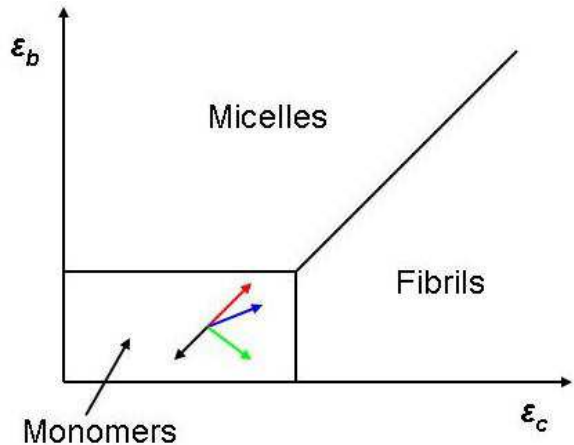
Finally, we compare the micellar and fibrillar species and we find that $f < \gamma_M$ if and only if:

$$\beta(\epsilon_c - \epsilon_b) > \log\left(\frac{\xi_b\nu_b\Theta_b s_b}{\xi_c\nu_c\Theta_c s_c}\right) + \beta P(v_c - v_b) . \quad (8)$$

The boundaries of the dominance diagram in terms of ϵ_b and ϵ_c are therefore all linear (c.f. Fig. 2). This may also be seen as a manifestation of the linear nature of the free energies assumed.

An immediate consequence of this investigation is that it provides a first-principle basis for the many empirical observations found in the literature [14, 15, 16, 17, 18, 19]. For instance, it is generally agreed that the following factors promote amyloid formation: i) an increase in hydrophobicity, and ii) an increase in length of an alternating hydrophobic-hydrophilic amino-acid sequence; while it is found that an increase in the number of charged amino acids decreases amyloid propensity. These effects are manifested in our discussion by considering their effects on ϵ_b and ϵ_c (c.f. the dominance diagram shown in Fig. 2). Specifically, an increase in hydrophobicity would increase both ϵ_b and ϵ_c and as such would on average increase the fibrillisation probability if the protein's parameters are already close to the monomer-fibril boundary in the dominance diagram (c.f. the red arrow in the Fig. 2). For our two-tape model for the amyloid fibril (c.f. Fig. 1c), an increase in alternating hydrophobic-hydrophilic amino-acid sequence would allow for packing the hydrophobic side chains inside the cross-beta sheet structure, while having the hydrophilic side chains outside, this would increase ϵ_c . On the other hand, having such a pattern would conceivably decrease the average energy gained inside a micellar structure given the amorphous structural nature, i.e., ϵ_b will be decreased. Such a modification would therefore increase amyloid propensity (c.f. the green arrow in the Fig. 2). If there is an increase in paired charges in the protein, i.e., charges that are not accompanied by ionic bonds, electrostatic interaction would deter aggregation and as such both ϵ_b and ϵ_c will be decreased (c.f. the black arrow in the Fig. 2).

FIG. 2: Dominance diagram of the three-species system at concentration higher than the critical concentrations if they exist. (C.f. Fig. 5 for how volume fractions vary as the concentration goes beyond the critical concentrations.) The coloured arrows depict how the dominance may shift under increase in hydrophobicity (red), increase in the number of aromatic side chains (blue), increase in alternating hydrophobic-hydrophilic amino-acid sequence (green), and increase in unpaired charges in the side chains (black).



Another insight we can gain from the above consideration concerns the importance of aromatic residues in amyloid propensity [7, 8, 9, 10, 11, 12, 13]. Beside the heightened hydrophobicity in aromatic residues, the off-set π -stacking interaction is directional along the fibrillar axis [38, 39], hence ϵ_c may be increased more than ϵ_b (c.f. the blue arrow in the Fig. 2). This suggests that aromatic interaction, or any interactions directional along the fibrillar axis, contributes to amyloid stability in a way different from ordinary hydrophobic interactions.

III. A QUANTITATIVE DISCUSSION

We will now attempt to make the above analysis more quantitative. We assume that the protein concerned has $L = 10$ amino acids, and we ignore the pressure terms for the time being, which is equivalent to saying that $v_a = v_b = v_c$. Our task is thus reduced to estimating the ratios as appeared inside the log in the inequalities in Eq. 6, 7 and 8.

Let us start with the ratio s_a/s_c , which corresponds to the relative configurational freedoms in monomeric proteins versus proteins in fibrils. We partition this ratio into two parts: the degrees of freedom from the peptide backbones and the degrees of freedom from the side-chains. For the peptide backbone, we estimate the ratio in the configurational freedoms by equating it to the ratio of the area occupied by an amino acid in the beta-sheet configuration and that of the total allowed area in the Ramachandran's plot (see, e.g., p. 113 in [40]). Specifi-

cally, we assume that the peptide backbone has only two degrees of freedom (rotations about the N-C $_{\alpha}$ bond and the C $_{\alpha}$ -C bond) per amino acid. By visual inspection of the Ramachandran's plot, we estimate that the area covered by the beta sheet configuration is about one half of the total allowed area. For the side-chain part, the degrees of freedom will be constrained in the fibrillar form in comparison to the monomeric species, and we assume that it contributes a factor of five to the overall ratio. In other words, $s_a/s_c \sim 10^L$. This estimate is consistent with the experimental data obtained in [41] and a similar estimate is adopted in [42]. For the micellar species, we expect that a monomer in a M -mer micelle is more constrained than the free monomers but less so than the monomers in fibrils. For the lack of a more accurate estimation, we assume that s_a/s_b is half of s_a/s_c . Namely, we have:

$$\frac{s_a}{s_b} = 5^L \quad , \quad \frac{s_a}{s_c} = 10^L . \quad (9)$$

We now turn to the ratios v_a/ν_b and v_a/ν_c , which relates to the translational freedoms of the different species. For the micellar species, we assume that the roaming space for each individual protein within the micelle is about 10% of the volume of the protein, we therefore have $v_a/\nu_b = 10$. For the fibrillar species, the proteins are packed more tightly and we assume that $v_a/\nu_c = 20$. In other words,

$$\frac{v_a}{\nu_b} = 10 \quad , \quad \frac{v_a}{\nu_c} = 20 . \quad (10)$$

The following ratios concern the rotational degrees of freedom. For the monomeric proteins and the proteins in the micellar species, we assume that they adopt the same configurations and that their moments of inertia are that of a uniform sphere, i.e.,

$$\Theta_a = \Theta_b = \left[\frac{2 \times \text{mass} \times (\text{radius})^2}{5} \right]^3 . \quad (11)$$

where the mass is about 100Lg/mol [43] and the radius is about $8\sqrt{L}\text{\AA}$ (assuming that the protein coils up like a free phantom chain with a persistence length of 20 \AA [43]). For the fibrillar species, the proteins adopt the beta-sheet configuration and for approximating its product moments of inertia, we assume that the beta strand can be approximated by a solid cylinder, i.e.,

$$\Theta_c = \frac{(\text{mass})^3 \times (\text{radius})^2 \times [3 \times (\text{radius})^2 + (\text{length})^2]^2}{288} , \quad (12)$$

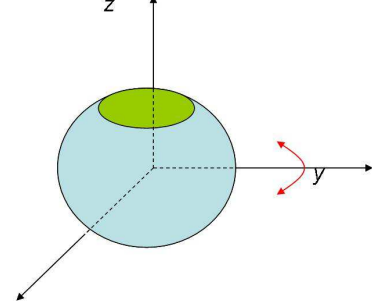
where the length is $3.25 \times L$ [40] and the radius of about 5 \AA (c.f. Fig. 4). We therefore find that for $L = 10$:

$$\frac{\Theta_a}{\Theta_c} \simeq 150 . \quad (13)$$

Hence for the rotational terms, we have:

$$\frac{\Theta_a}{\Theta_b} = 1 \quad , \quad \frac{\Theta_a}{\Theta_c} = 150 . \quad (14)$$

FIG. 3: A schematic depicting the angular constrain with respect to the centre of mass of a protein within a micelle. The green patch on top shows the angular restriction on the z -axis (assumed to be $\sim 10\%$ in area in comparison to the whole area of the sphere) and red arrow shows the angular constraint on picking the y -axis (again assumed to be $\sim 10\%$ of a complete rotation).



The last terms we need to be concerned with are the angular restrictions (c.f. the Appendix). Note that any coordinate frame is determined by fixing the two of the axes, x and y axes, say. For the micellar case, a monomer in a M -mer micelle is not free to rotate completely and we assume that the rotational freedom is 1% of that of a monomeric protein (c.f. Fig. 3), i.e., $\xi_b = 0.01$. For the fibrillar case, we assume that in order to maintain the hydrogen bonds along the beta strand, the end points of the beta strand can only fluctuate for no more than 0.2 \AA (c.f. Fig. 4), this leads to:

$$\frac{\theta^2}{4} = \frac{1}{4} \times \left[\sin^{-1} \left(\frac{0.2}{3.25L/2} \right) \right]^2 \simeq 3.8 \times 10^{-5} . \quad (15)$$

Furthermore, we assume that the rotation allowed around the axis along the beta sheet to be about 10% of the a complete rotation. In other words,

$$\xi_b = 0.01 \quad , \quad \xi_c = 3.8 \times 10^{-6} . \quad (16)$$

We now take M to be 30 [24], and L to be 10 as before. Since we know that the critical concentrations for amyloid formation in physiologically relevant systems are in the μM range, we require that the critical concentration for fibrillar formation is in the range of $10\mu\text{M}$ here (e.g. [5]). The volume per amino acid of a typical protein is about 100\AA^3 [43], the critical volume fraction is therefore 6×10^{-6} for a 10-amino-acid protein. Combining the estimated ratio in Eq. 9, 10, 14 and 16, we find that the inequalities in Eqs. 6 and 8 become:

$$\beta\epsilon_c > 43.5 + \underline{12} \quad , \quad \beta(\epsilon_c - \epsilon_b) > 20.5 , \quad (17)$$

where the underlined term in the first inequality results purely from requiring that the critical concentration is at $10\mu\text{M}$. From the above inequalities, we see that fibrils are the dominant species if $\epsilon_c/L > 5.6k_B T \simeq 3.3\text{kcal/mol}$ at

FIG. 4: A schematic depicting the angular constrain with respect to the centre of mass of a beta strand, shown as a solid cylinder, within a three-protein cross-beta structure.

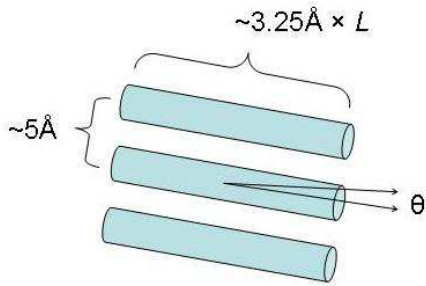
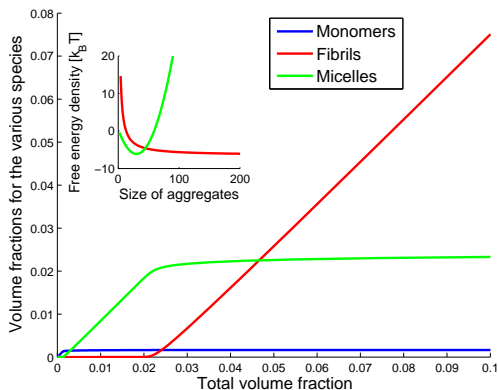


FIG. 5: The volume fractions for the various species for the system discussed in Section III, with $\beta\epsilon_b = 28.9$ and $\beta\epsilon_c = 50$. The inset plot show the free energy densities, with η set to zero.



room temperature. Given that a hydrogen bond in solution is about 1.5kcal/mol [44] and that each amino-acid on average contributes two hydrogen bonds in a fibril, the energy contribution from side-chains is paramount in order for stable fibrillar formation. This explains why fibrils are usually in the form of stacks of cross-beta structure, as our analysis suggests that a single sheet is unlikely to be energetically stable for amyloid formation. From the above inequalities, we also learn that the fibrillar phase will be dominant only if $(\epsilon_c - \epsilon_b)/L > 2.1k_B T \simeq 1.3\text{kcal/mol}$ at room temperature. This is remarkably close to the energy gained from hydrogen bonding, which suggests that our model protein is close to the boundary in the dominance diagram. We believe that this provides a reason for the relative ease in inducing protein amyloid formation in laboratories, e.g., by varying the temperature, the pressure or the salt concentration (which has the effect of shifting the hydrophobic interactions).

IV. MODEL EXTENSIONS

A. Inclusion of native structure

Most proteins have well defined native states, or at least stable domains. It has also been demonstrated that on average, each amino acid contributes $\sim 0.2 \times k_B T$ to the stability of the native structure [43]. In other words, denoting the free energy density of a protein with a native structure by η' , we can say that $\eta' \simeq \eta - 0.2 \times L k_B T$ where η is the free energy as before and L is the number of amino acids. The inequality in Eq. 6 is therefore modified to:

$$\beta(\epsilon_c - 0.2 \times L) > \log \left(\frac{v_a \Theta_a s_a}{\xi_c \nu_c \Theta_c s_b} \right) + \beta P(v_c - v_a). \quad (18)$$

Namely, the threshold bonding energy for amyloid fibril formation is increased by $0.2k_B T$ per amino acid. Although the change seems small, it is in fact a stringent requirement as the native structure is likely to be stabilised by a networks of ionic, covalent (e.g., sulfur-sulfur) and hydrogen bonds besides the usual hydrophobic interactions, and therefore would be unlikely to be retained in the fibrillar structure.

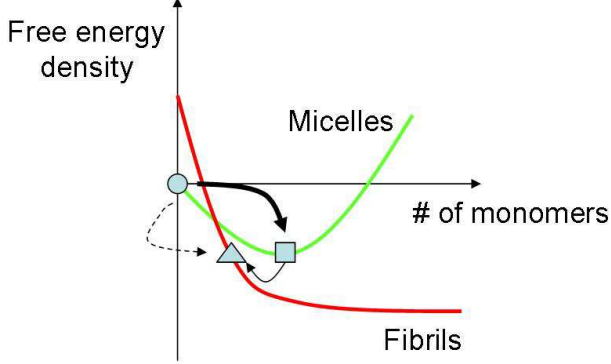
B. Effect of pressure

Pressure has an important effect on amyloid formation (see [45] and the references therein), which is manifested by the fact that the solution is not a continuum and as such, cavities exist. As it is generally agreed that amyloid fibrils are structurally similar [2, 4], we assume here that in a fibril, each residue group occupies a volume of $3.25 \times 10 \times 5 = 163 \text{\AA}^3$. Since we also know that a residue group contributes on average $1.97 \times 10^{-22} \text{g}$ [46], the average density for a fibril is therefore approximately 1.21g/cm^{-3} . In comparison, the average density of a protein is around 1.35g/cm^{-3} [47]. It therefore suggests that an increase in pressure will generally promote fibrillisation. Along the same line of reasoning, proteins with large side chains will also have a greater ease at fibrillising (c.f. the last term in Eq. 6). In particular, as aromatic residues tend to have higher volumes, this provides another reason for its role in promoting amyloid formation.

V. KINETICS

We now discuss how the picture developed in this paper helps to describe the kinetics of the self-assembly process. Following the theory proposed in [48], the series of events leading up to the fibrillisation of amyloid- β proteins is depicted in Fig. 6 (c.f. the caption). In this scenario, the direct pathway from monomers to stable nucleus (depicted by the broken arrow in Fig. 6) is in a

FIG. 6: A schematic digram depicting the amyloid-beta self-assembly process proposed in [48]. The circle denotes the free monomeric state, the square denotes the typical micellar state, and the triangle denotes a stable nucleus. The thick arrow depicts the fast pathway from free monomer to micelles and the thin arrow depicts the slow process of nucleation from micelles. The broken arrow depicts that very slow process of nucleation from free monomers, which is out of the range of experimental time scale, but may play an important role in actual pathogenesis under physiological time scale.



time scale too long to be probed experimentally. Therefore, the only possible fibrillisation pathway is for the monomers to first formed micelles (a fast process, depicted by the thick black arrow), stable nuclei are then formed out of the micelles (a slow process, depicted by the thin black arrow). As mentioned before, there are two critical concentrations, one associated to micelle formation and the other to fibril formation, the current picture indicates that in the experimental time scale, the concentration has to be beyond the CMC which is in the range of 0.1mM. Since the concentration of amyloid-beta in the cerebral spinal fluid is only in the subnanomolar concentration range [49], the important message here is that our experimental methods may be probing the fast pathway only – monomers to micelles to nucleus (depicted by the two solid arrows), while the physiologically relevant pathway is the slow pathway – monomers to nucleus (depicted by the broken arrow).

VI. CONCLUSION

In this work, we have considered the thermodynamic equilibrium behaviour of a system with a mixture of monomeric proteins, the corresponding micellar aggregates and fibrillar aggregates by carefully investigating the entropic and energetic components of the various species. In the process, we gain an understanding of the empirical observations from first principles, such as the

amyloid propensity factors and the structural details. In particular, we found that aromatic residues contribute to amyloid formation in three different manners: i) high hydrophobicity, ii) π -stacking interaction along the fibrillar axis, and iii) high volume. Although these reasons have been in discussion in the literature, we believe that in this work, they are introduced from first principles and are also treated in a more coherent manner. Moreover, by incorporating physiologically relevant parameters into our toy model, we explained why it is of relative ease to induce amyloid formation in many proteins and why it is energetically important for having multi-layer cross-beta structures. Our analysis also provides insight on the kinetic process in amyloid formation.

Acknowledgments

The author thanks the Glasstone Trust (Oxford) and Jesus College (Oxford) for financial support.

APPENDIX A: FREE ENERGY DENSITY CALCULATIONS

For a polydisperse aggregation system with a total of N proteins in a solution of volume V , the canonical partition function is:

$$Z = \sum'_{l, \{m_h\}, \{n_k\}} \prod_{l, h, k} \frac{1}{l! h! m_h! k! n_k!} A^l (B_h)^{m_h} (C_k)^{n_k} \quad (\text{A1})$$

where l , m_h and n_k denote the numbers of monomers, h -mer micelles and k -mer fibrils respectively, and

$$A = \int [dp][dr] e^{-\beta H^a(\{p\}, \{r\})}, \quad (\text{A2})$$

$$B_h = \int [dp_h][dr_h] e^{-\beta H_h^b(\{p_h\}, \{r_h\})}, \quad (\text{A3})$$

$$C_k = \int [dp_k][dr_k] e^{-\beta H_k^c(\{p_k\}, \{r_k\})}. \quad (\text{A4})$$

where, e.g., $\int [dp_k]$ signifies integrating over all of the atoms' momenta in a k -aggregate fibril, and the H^a , H_h^b and H_k^c are the hamiltonians for the monomeric, h -mer micellar and k -mer fibrillar species. To conserve the total number of proteins, the prime in the sum in Eq. A1 signifies that the sum is over all l , m_h and n_k such that

$$l + \sum_{h \geq 2} h m_h + \sum_{k \geq 4} k n_k = N, \quad (\text{A5})$$

where the sum starts at $k = 4$ in the third term because a four-segment fibril is the smallest fibrillar structure in our model (c.f. Fig. 1c).

At the thermodynamic limit, we ignore fluctuations in l , m_h and n_k , hence the above partition function reduces

to

$$Z = \prod_{l,h,k} \frac{1}{l! h! m_h! k! n_k!} A^l (B_h)^{m_h} (C_k)^{n_k} . \quad (\text{A6})$$

With the expression of the partition function at hand, we are now ready to obtain the Gibb's free energy density (i.e., the Gibb's free energy per protein) for the various aggregation species.

1. Monomers

As a first approximation, we ignore interactions between the protein and solution as well as between the distant parts of the protein. Therefore, A has only entropic contributions and they can be partitioned into three parts: translational, rotational and configurational. In other words, we obtain for A [50]:

$$A = \underbrace{\kappa V}_{\text{translation}} \times \underbrace{\omega \Theta_a}_{\text{rotation}} \times \underbrace{s_a}_{\text{configuration}} , \quad (\text{A7})$$

where all three terms are dimensionless. The translational term corresponds to the translational freedom for the centre of mass of the protein, with [50]

$$\kappa = \left(\frac{2\pi m}{\beta h^2} \right)^{3/2} , \quad (\text{A8})$$

where m is the mass of the protein and h is the Planck's constant. The rotational term corresponds to the rotational freedom of the protein with respect to its center of mass, with

$$\omega = \frac{16\sqrt{2}\pi^{3/2}}{\beta^{3/2}h^3} , \quad \Theta_a = I_x I_y I_z , \quad (\text{A9})$$

where ω corresponds to the kinetic contribution from the angular momentum and the $I_{\{x,y,z\}}$ are the principle moments of inertia for the protein [50]. The last term in Eq. A7 corresponds to the translational freedom of all the atoms in the protein once any three non-colinear atoms coordinates are fixed. The latter restrictions are to discount for the translational and rotational degrees of freedom already considered.

With the expression for A , the monomer's chemical potential density can be easily calculated to be:

$$\mu^a = -\frac{1}{\beta} \frac{\partial}{\partial l} (\log Z - \beta P V) = -\frac{1}{\beta} (\log A - \log l - \beta P v_a) , \quad (\text{A10})$$

where P is the pressure exerted on the system, and

$$V = V_s + l v_a + \sum_{h \geq 2} h m_h v_b + \sum_{k \geq 4} k n_k v_c , \quad (\text{A11})$$

with V_s being the volume of the solution without the proteins. As the interesting regime of concentration for

protein amyloid formation is at the μM level, V is always very close to V_s . Denoting now the volume fraction of the monomers by $X^a = \frac{l v_a}{V}$ where v_a is the volume of the protein, the monomer's chemical potential density becomes:

$$\mu^a = -\frac{1}{\beta} [\log A - \log X^a - \log(V/v_a) - \beta P v_a] . \quad (\text{A12})$$

By substituting our expression in Eq. A7 to the above equation, we obtain:

$$\mu^a = \eta + \frac{1}{\beta} \log(X^a) \quad (\text{A13})$$

where the monomer's free energy density, η , is:

$$\eta = -\frac{1}{\beta} [\log(\kappa v_a) + \log(\omega \Theta_a) + \log(s_a) - \beta P v_a] . \quad (\text{A14})$$

2. Micelles

In the micellar case, B_k can again be expressed as:

$$B_M = \underbrace{\kappa^M V \nu_b^{M-1}}_{\text{translation}} \times \underbrace{\omega^M \Theta_b^M \xi_b^{M-1}}_{\text{rotation}} \times \underbrace{s_b^M}_{\text{configuration}} \times \underbrace{e^{M \epsilon_b}}_{\text{bonding energy}} \quad (\text{A15})$$

where the translation term contains contributions from the translational freedoms of the centre of mass of the whole aggregate, i.e., the factor κV , as well as from the translational freedoms for the centre of mass of each individual protein in the aggregate, i.e., the factor $(\kappa \nu_b)^{M-1}$, where ν_b designates the restricted space that each monomer is allowed to roam within the micelle. Note that the κ here is the same as in Eq. A8, which is due to the fact that ϵ_b is always higher than a few $k_b T$ and as such we have approximated the integrals over the kinetic parts by extending the limits of the momenta integrals to infinity. The same applies to the rotational term with ξ_b denoting the restriction on the rotational freedom. For the configurational term, we assume that each protein in the aggregate is completely independent of each other and each one has the same configurational freedom. The one distinction from the monomeric species is that B_M is now supplemented by a bonding energy term which reflects the average gain in stability, e.g., by hydrophobic interactions per protein in the aggregate.

Similar to Eq. A10, the chemical potential density is:

$$\mu_M^b = -\frac{1}{\beta} [\log(B_M) - \log(m_M) - \beta P M v_b] , \quad (\text{A16})$$

where m_M is the number of M -mer micelles. Expressing it in terms of volume of fraction, $X_M^b \equiv m_M M v_b / V$, we have:

$$\mu^b = \gamma_M + \frac{1}{\beta M} \log \left(\frac{X_M^b}{M} \right) \quad (\text{A17})$$

where the optimal micellar free energy density is:

$$\gamma_M = -\frac{1}{\beta M} \left\{ \log [\kappa^M v_b \nu^{M-1}] + \log [\omega^M \Theta_b^M \xi_b^{M-1}] + M\beta\epsilon_b + M \log(s_b) - \beta P M v_b \right\}. \quad (\text{A18})$$

Note importantly that the average volume of a protein a M -mer micelle, v_b , may differ from the volume of a free protein in solution, v_a . This is because the solution is not a perfectly filling continuum.

3. Fibrils

As in the micellar case, C_k can be expressed as:

$$C_k = \underbrace{\kappa^k V \nu_c^{k-1}}_{\text{translation}} \times \underbrace{\omega^k \Theta_c^k \xi_c^{k-1}}_{\text{rotation}} \times \underbrace{s_c^k}_{\text{configuration}} \times \underbrace{e^{(k-2)\epsilon_c}}_{\text{bonding energy}}, \quad (\text{A19})$$

where ν_c is, similarly to the micellar case, the restricted space that each protein can roam within a fibril, and ϵ_c is the energy gained from hydrogen bonding, hydrophobic interactions, etc, per protein by being part of a fibril. Note the factor $(k-2)$ in front of ϵ_c , which is due the assumption that the fibril consists of two layers of cross-beta structure with contributions from the two ends subtracted.

For the fibrillar species, the chemical potential densities are:

$$\mu_k^c = f_k + \frac{1}{\beta k} \log \left(\frac{X_k^c}{k} \right) \quad (\text{A20})$$

where the fibrillar free energy densities are:

$$f_k = -\frac{1}{\beta k} \left\{ \log [\kappa^k v_c \nu_c^{k-1}] + \log [\omega^k \Theta_c^k \xi_c^{k-1}] + (k-2)\beta\epsilon_c + k \log(s_c) - \beta P k v_c \right\}. \quad (\text{A21})$$

4. Relative volume fractions

At thermal equilibrium, the above chemical potential densities for all of the various species: monomers, micelles and fibrils, are identical and we can express the various volume fractions in terms of the monomer volume fraction, X^a (e.g., see [37]), which gives:

$$X_h^b = h \left(X^a e^{\beta(\eta - \gamma_h)} \right)^h, \quad (\text{A22})$$

$$X_k^c = k \left(X^a e^{\beta(\eta - f_k)} \right)^k. \quad (\text{A23})$$

There are therefore two critical concentrations, one for the micellar species and one for the fibrillar species. As $h, k \gg 1$, the species with the lowest free energy density will dominate at concentration above the higher of the two critical concentrations.

-
- [1] M. Sunde et al., J. Mol. Biol. **273**, 729 (1997).
 - [2] C. M. Dobson et al., Nature **426**, 905 (2003).
 - [3] S. E. Radford, Trends in Biochemical Sciences **25**, 611 (2000).
 - [4] M. R. Sawaya et al., Nature **447**, 453 (2007).
 - [5] J. D. Harper and P. T. Lansbury, Jr., Annu. Rev. Biochem. **66**, 385 (1997).
 - [6] T. Schelbel et al., PNAS **100**, 4527 (2003).
 - [7] M. Reches et al., J. Biol. Chem. **277**, 34575 (2002).
 - [8] M. Reches et al., Science **300**, 625 (2003).
 - [9] S. M. Tracz et al., Biochem. **43**, 15901 (2004).
 - [10] B. Ma and R. Nussinov, Curr. Opin. Chem. Biol. **10**, 445 (2006).
 - [11] F. Bemporad et al., Protein Science **15**, 862 (2006).
 - [12] P. Marek et al., Biochem. **46**, 3255 (2007).
 - [13] L. Jean, C. F. Lee, M. Shaw, and D. J. Vaux, PLoS ONE **3**, e1834 (2008).
 - [14] S. Yoon and W. J. Welsh, Protein Science **13**, 2149 (2004).
 - [15] A.-M. Fernandez-Escamilla et al., Nature Biotechnology **22**, 1302 (2004).
 - [16] G. G. Tartaglia et al., Protein Science **14**, 2723 (2005).
 - [17] O. X. Galzitskaya et al., PLoS Comp. Biol. **2**, 1639 (2006).
 - [18] K. F. Dubay et al., J. Mol. Biol. **341**, 1317 (2004).
 - [19] A. P. Pawar et al., J. Mol. Biol. **350**, 379 (2005).
 - [20] J. F. Smith et al., PNAS **103**, 15806 (2006).
 - [21] T. P. J. Knowles et al., Phys. Rev. Lett. **96**, 238301 (2006).
 - [22] T. P. J. Knowles et al., Nanotechnology **18**, 044031 (2007).
 - [23] T. R. Serio et al., Science **289**, 1317 (2000).
 - [24] W. Yong et al., PNAS **99**, 150 (2002).
 - [25] H. D. Nguyen and C. K. Hall, PNAS **101**, 16180 (2004).
 - [26] R. Pellarin and A. Caffisch, J. Mol. Biol. **360**, 882 (2006).
 - [27] P. H. Nguyen et al., PNAS **104**, 111 (2007).
 - [28] R. Pellarin et al., J. Mol. Biol. **374**, 917 (2007).
 - [29] M. Cheon et al., PLoS Comput. Biol. **3**, e173 (2007).
 - [30] W.-F. Xue et al., PNAS **105**, 8926 (2008).
 - [31] J. van Gestel and S. W. de Leeuw, Biophys. J. **90**, 3134 (2006).
 - [32] A. Aggeli et al., PNAS **98**, 11857 (2001).
 - [33] I. A. Nyrkova et al., Eur. Phys. J. B **17**, 499 (2000).
 - [34] G. Tian et al., J. Chem. Phys. **120**, 8307 (2004).

- [35] N. Guex and M. Peitsch, *Electrophoresis* **18**, 2714 (1997).
- [36] J. L. Jiménez et al., *PNAS* **99**, 9196 (2002).
- [37] R. A. L. Jones, *Soft Condensed Matter* (Oxford University Press, Oxford, 2002).
- [38] C. A. Hunter et al., *J. Mol. Biol.* **218**, 837 (1991).
- [39] E. A. Meyer, R. K. Castellano, and F. Diederich, *Ange wandte Chemie* **42**, 1210 (2003).
- [40] M. Daune, *Molecular Biophysics: Structures in motion* (Oxford University Press, Oxford, 1999).
- [41] J. F. Brandts, *J. Am. Chem. Soc.* **86**, 4302 (1964).
- [42] J. D. Bryngelson and P. G. Wolynes, *Proc. Natl. Acad. Sci. USA* **84**, 7524 (1987).
- [43] K. Sneppen and G. Zocchi, *Physics in Molecular Biology* (Cambridge University Press, Cambridge, 2005).
- [44] S.-Y. Sheu et al., *PNAS* **100**, 12683 (2003).
- [45] T. W. Rabdolph et al., *Biochimica et Biophysica Acta* **1595**, 224 (2002).
- [46] A. A. Zamyatnin, *Ann. Rev. Biophys. Bioeng.* **13**, 145 (1984).
- [47] H. Fischer et al., *Protein Science* **13**, 2825 (2008).
- [48] A. Lomakin et al., *PNAS* **94**, 7942 (1997).
- [49] P. Seubert et al., *Nature* **359**, 325 (1992).
- [50] T. L. Hill, *An Introduction to Statistical Thermodynamics* (Dover, New York, 1986).